"Long Plan" - One-Family, Solar Powered house for the "Solar Decathlon China - 2018" Competion, Dezhou (China). Winning Project

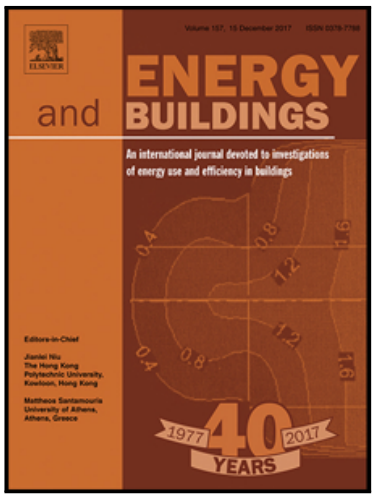

Optimizing the transition between design and operation of ZEBs:lessons learnt from the Solar Decathlon China 2018 SCUTxPoliTo Prototype

Maria Ferrara , Ciro Lisciandrello , Alessio Messina , Mauro Berta , Yufeng Zhang , Enrico Fabrizio

PII: S0378-7788(19)32080-8
DOI: https://doi.org/10.1016/j.enbuild.2020.109824
Reference: ENB 109824

To appear in: *Energy & Buildings*

Received date: 17 July 2019
Revised date: 24 January 2020
Accepted date: 28 January 2020

Please cite this article as: Maria Ferrara , Ciro Lisciandrello , Alessio Messina , Mauro Berta , Yufeng Zhang , Enrico Fabrizio , Optimizing the transition between design and operation of ZEBs:lessons learnt from the Solar Decathlon China 2018 SCUTxPoliTo Prototype, *Energy & Buildings* (2020), doi: https://doi.org/10.1016/j.enbuild.2020.109824

Optimizing the transition between design and operation of ZEBs: lessons learnt from the Solar Decathlon China 2018 SCUTxPoliTo Prototype

Maria Ferrara[a], Ciro Lisciandrello[a], Alessio Messina[a], Mauro Berta[b], Yufeng Zhang[c], Enrico Fabrizio*[a]

[a]*DENERG- TEBE Research Group, Politecnico di Torino, Corso Duca degli Abruzzi 24, 10129 Torino, Italy*

[b]*DAD - China Room, Politecnico di Torino, Corso Duca degli Abruzzi 24, 10129 Torino, Italy*

[c]*South China University of Technology, Wushan Road, Tianhe District, Guangzhou, P.R.C.*

Abstract

In the context of the worldwide efforts to reduce energy consumptions and carbon dioxide (CO_2) emissions related to the building sector, reaching the high performance of a zero energy building (ZEB) has been demonstrated to be feasible, especially when the design phase is supported by integrated simulation-based optimization methods. It is necessary to pay special attention to the transition from building design to building operation and it is hard to find examples of real ZEB buildings where the that are optimized considering design and operation at the same time. In this context, the Solar Decathlon competition is a unique experimental field to advance in research about design, simulation, and optimization of ZEBs.

This study aims at presenting the energy-related scientific aspects behind and beyond the winner building prototype of the Solar Decathlon China 2018 competition. An optimization-based calibration supported by sensitivity analysis is carried out to calibrate the simulation model of the ZEB prototype, based on data collected throughout the design and construction phase. Then, an original simulation-based optimization method is tailored to the purpose of maximizing the contest score, considering parameters related to both design and operation of the building.

A high level of model calibration was reached, and the contest score was improved by 15 points, helping the ZEB prototype to win the competition. Results demonstrated that the applied methodological framework was able to drive towards optimized and integrated design and operation strategies.

Keywords: Solar Decathlon; Integrated design; simulation; calibration; optimization; TRNSYS; GenOpt, Matlab; sensitivity analysis; simulation-based optimization

* Corresponding author. Phone: +39 0110904465. E-mail: enrico.fabrizio@polito.it

Nomenclature

Acronyms

BEM	building energy model
CSM	case study model
ERV	energy recovery ventilator
GPS	generalized pattern search
OSB	oriented strand board
PSO	particle swarm optimization
SA	sensitivity analysis
SBOM	simulation-based optimization method
TMY	typical metereological year
VIP	vacuum insulation panel
VRV	Variable refrigerant volume
ZEB	Zero Energy Building

Variables and quantities used in equations

CO_2	carbon dioxide
Cv(RMSE)	coefficient of variation of the root mean square error
EB	energy balance
EE	elementary effect
NMBE	normalized mean bias error
$P_{CO2,i}$	contest points related to CO_2 in the timestep i
P_{EB}	contest points related to *EB*
$P_{PM2.5,i}$	contest points related to *PM2.5* in the timestep i
$P_{RH,i}$	contest points related to *RH* in the timestep i
$P_{T,i}$	contest points related to *T* in the timestep i
PM2.5	particulate matter that have diameter equal or less than 2.5 micrometers
RH	relative humidity
T	indoor air temperature

μ_i	mean value
μ_i^*	absolute mean value
σ_i	standard deviation
τ	total number of evaluated time-steps in the contest period

1. Introduction

In the context of the worldwide efforts to reduce energy consumptions and carbon dioxide (CO_2) emissions related to the building sector, the concept of zero energy building (ZEB) has emerged as the main driver towards these objectives [1]. Whatever are the metrics used to assess its performance, it has been proved that reaching the ZEB target can be technically feasible [2], especially when the design phase is supported by integrated simulation-based optimization methods that are able to predict in details the building energy performance and to optimize it within a design space composed of a large amount of design alternatives [3].

A traditional parametric design approach may lead to spend and waste a lot of time on useless design variables. If all the important design variables are not considered and the mutual relationship between them is not taken into account, it could lead even non-optimal solution [4]. It is recognized that simulation-based methods are powerful tools for effectively solving this kind of complex problems while saving time [5]. In fact, they help reduce the high computational cost needed to check a great number of design alternatives while ensuring a considerable accuracy in finding the optimal design solution [6].

In building science, such simulation-based optimization methods have been applied to many different problems, like energy consumption reduction [7], increase of the efficiency of systems [8], indoor comfort evaluation and optimization [9], and mostly on the cost optimization with a life cycle perspective [10][11]. If most of these studies are performed to optimize the building design, others focus on the building operation to optimize its control strategies [12][13][14]. It is hard to find examples of real ZEBs that are optimized using a simulation-based optimization method considering parameters related to design and operation at the same time.

However, special attention has to be paid to the transition from building design to building operation, considering that the availability of reliable energy models has been proved to be effective in supporting not only the design phase, but also the building operation phase, thus contributing to reduce the "performance gap" [15] often occurring between the predicted performance at the design stage and the performance of the building after construction. To do so, it is necessary to calibrate the energy model based on monitored data, in order to perform the required "tuning" of the model to fit its behavior to the actual building behavior [16]. It is known that there are several methods for building model calibration, from manual calibration to graphical-based calibration methods, from calibration based on special tests and analysis procedures to automated techniques for calibration based on analytical and mathematical approaches. Since the first introduction of this classification [17], many studies were published

about applications and advancements related to either methods. In the last few years, the increasing effectiveness of simulation-based optimization methods (SBOM) tailored for the ZEB design process [18] has led to increasing interest in studying the application of the same methods to building model calibration. When compared to manual methods for calibration, such optimization-based calibration method presents some advantages. In fact, they do not rely on the experience of the user to carry on the optimization but on a solid mathematical structure. Moreover, the computational time is highly reduced at the same level of exploration of the viable solutions [19]. In order that these advantages are fully exploited, the users have to be really precise in selecting input parameters and optimization method. The choice could be guided through a Sensitivity Analysis (SA). The SA will actively explore the hyperspace of possible solutions and rank the parameters accordingly to their influence on the final outcome [20].

In view of the above, the use of SBOM within the ZEB design process appears to be promising, but their ability to effectively support the ZEB reliable modelling and lead to an optimized transition from design to operation still have to be tested. The fact that it is hard to find studies dealing with this problem may be due to the difficulties in finding case studies and project boundaries that are suitable for this purpose. It is even harder to find opportunities to test and validate the most advanced simulation and optimization methods in practice, experimenting their ability to follow and support the entire design-construction-management process of a real ZEB.

In this context, the Solar Decathlon competition is a unique opportunity to advance in research in the field of ZEB design. Solar Decathlon is a worldwide engineering and architecture challenge in which the different teams, composed of students and advised by researchers from technical universities, have to design, build and operate a ZEB [21].

In fact, the integrated process from design to construction that is carried out for the competition purposes, the advanced required monitoring systems, the large amount of collected data and the highly interdisciplinary team working together from design to construction constitutes a fertile base for research that is hard to find in other contexts.

Since the first edition, which took place in Washington D.C. in 2002, the main purpose of Solar Decathlon is to put together teams of students with architectural and engineering backgrounds to give life to a real residential ZEB prototype. The contest is based on ten sub-contests, where the teams need to achieve the highest possible score to win the competition. The total score is 1000 points, divided into 100 points for each sub-contest. Five of them investigates the project, the documentation, and the systems (Architecture, Market Appeal, Engineering, Communication, Innovation - subjected to a jury review), while the other five focus on measured parameters, related to the comfort of occupants, the efficiency of the systems, and the energy

production (Comfort Zone, Appliances, Home Life, Commuting, Energy). So, the ZEB is judged on a complex system of parameters characterizing its performance and its livability. There are a lot of design-related and operation-related involved parameters, each one may impact at the same time energy consumption and production, comfort, operation time.

In particular, the measured ones need to be maintained in a certain range in order to lower as much as possible the energy consumption while optimizing the stability and the efficiency of the systems and ensuring the occupants' comfort is maximized. Therefore, the design of the ZEB prototype can be seen as a complex optimization problem, where the Solar Decathlon final contest score may be seen as the objective function to be maximized.

In August 2018, thanks also to the application of simulation-based optimization methods throughout the entire design and construction phases, a team composed of students from Politecnico di Torino and the South China University of Technology (SCUT-POLITO team) won the Solar Decathlon China competition. We believe it is worth presenting and analyzing in detail the scientific approach behind and beyond such a successful experience.

1.1. Motivation and approach

Based on the Solar Decathlon context, this work provides insights on the design, modelling and optimization of a real residential ZEB prototype. It constitutes an innovative experimental study on the use of building simulation and optimization to support a real building design-construction-operation process, aiming at highlighting strengths and weaknesses of the use of such advanced research tools within a real set of time and physical constraints.

Through the setup of an integrated simulation-based optimization framework, the approach is composed of two main steps.

The first step is the creation of a highly reliable simulation model that is capable to predict the behavior of the envelope and consequently simulate the performance of systems in details. This offers a unique opportunity to investigate and test innovative research approaches for real model calibration. As mentioned, the integrated process from design to construction and operation and the easiness of collecting a large amount of data constitutes a fertile base for research that are hard to find in other contexts. The first objective is therefore to propose a multi-step optimization-based calibration of the model of a ZEB prototype that is reached through the following sub-steps, each constituting a sub-objective:

- setting up a simulation-based optimization framework able to calibrate the performance of a ZEB building;

- carrying out a complete SA based on an optimized Morris Method to improve the efficiency of the framework;
- testing the method on the real ZEB prototype;
- evaluating the impact of the use of this method within and outside the context of the Solar Decathlon competition.

The second step, which constitutes the final objective, is the combination of design and operational optimization of the ZEB prototype, based on the previously calibrated Building Energy Model (BEM). This is reached through the following sub-steps, each constituting a sub-objective:

- Implementation of the Contest Schedules;
- Definition of the objective function based on the Solar Decathlon competition rules;
- Setup of a simulation-based optimization framework able to optimize the performance of the resulting ZEB building (coupling of TRNSYS, MATLAB, GenOpt);
- Design variation on the base of the results and evaluate the impact of the use of this method within the Solar Decathlon competition and for real ZEB design, construction and management processes.

The structure of the paper reflects the presented multi-step approach. After a short description of the building concept and of the prototype features, both the method and the results are organized into two main subsections referring to the optimization-based model calibration and to the combined design and operation optimization, respectively. It has to be remarked that, in order that the approach is clear to the reader, these two steps are presented following a logical order that does not necessarily correspond to a strict chronological order of the work process. The fact that in this work simulation and optimization are experimentally used to support a real design and construction process is crucial. In fact, in presence of bad results obtained from first simulations at the design stage and of new constraints emerging at the construction stage, the different steps were performed several times, sometimes iteratively, always supported by a re-calibrated simulation model, to reshape the building design and its optimized operation strategies. In addition to the previous observations, it should also be noted that the construction of the building prototype was performed two times in two different locations, one during the contest preparation (Guangzhou) and the other in the final contest location (Dezhou).

1.2. The LONGPLAN prototype

In order to deal with the land-take problem, which is dramatically growing in China in the last years, the LONG PLAN ZEB prototype (Figure 1) is meant to reach a significantly higher density in relation to the traditional one familiar detached houses, which are usually the reference typologies in the Solar Decathlon proposals. Thus, it is based on the "narrow house" typology, which is very common both in the traditional South China dwellings (Lingnan houses) and in the European history (terraced houses) as well as in many other cultures, and which can be summarized with the "low rise, high density" concept. The built prototype is just a single unit that could be either used as an individual building to infill existing fabrics, or as a reproducible model to be replicated and customized in order to generate new neighborhoods for a wider market.

Figure 1: The LONG PLAN house during construction (top) and at the end of construction (bottom)

The building has a modular steel structure with 12 pre-fabricated modules. The walkable area of the two floors is about 143 m^2. The building plans, reported in Figure 2, can be divided into three main sectors:

- *Integrated Wall*: The west-side external wall, which contains all the distribution pipes for hot water, coolant, DHW and all the electrical and electronic connection. This allows limiting the use of space while facilitating maintenance;

- *Service Belt*: A narrow "slice" of the building that includes all the services and systems. Here lay the stairs, the three bathrooms, the mechanical room, the aquaponic system and the kitchen appliances;
- *Living Belt*: This section is composed of the 4 conditioned zones: living room, kitchen and the two bedrooms, connected by one corridor for each floor that is adjacent to a central patio. This space is delimited by a green wall on the external side and an automated window on the roof that are devoted to improving passive strategies, such as the reduction of solar gains and the chimney effect.

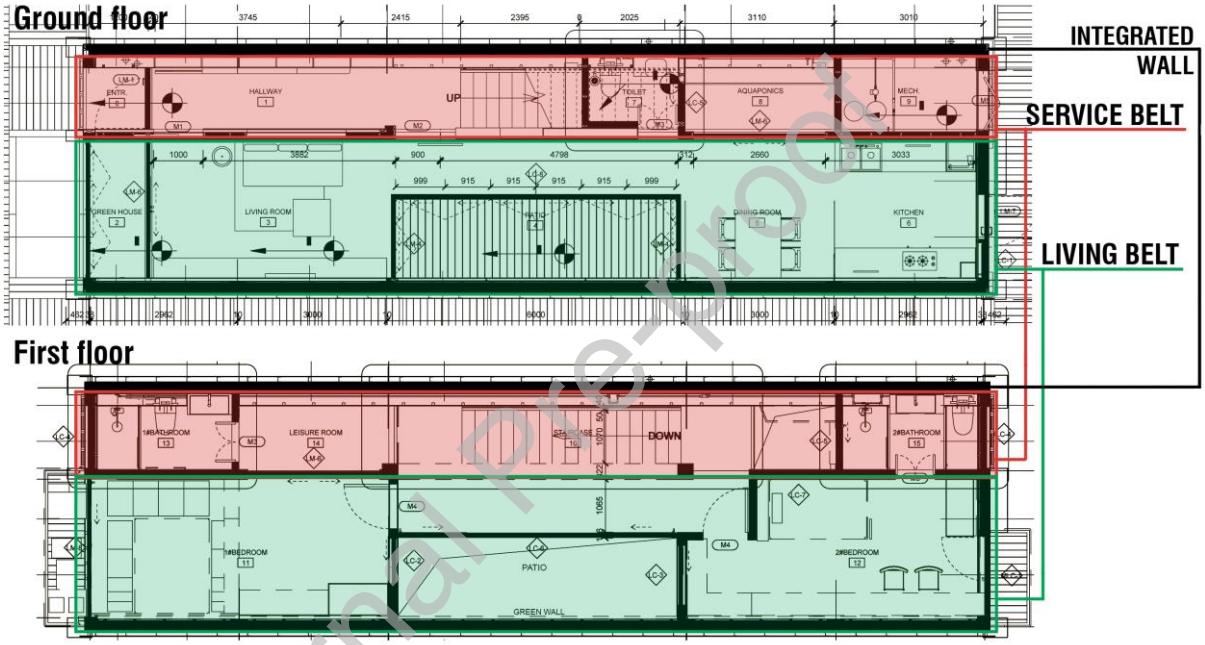

Figure 2: The LONG PLAN plans of ground floor (top) and first floor (bottom)

Transparent envelope (U_w ranging from 0.8 W/m^{2}K to 1.2 W/m^{2}K) is only on North and South facades (shortest sides), plus two skylights near the staircase, because the longest walls are conceived to be adjacent to the other houses. The opaque envelope is composed of OSB (Oriented Strain Board) panels, VIP (Vacuum Insulated Panels), phenolic insulation, water barrier, vapor barrier (roof and walls: U=0.095 W/m^{2}K; ground slab: U=0.129 W/m^{2}K). The east and west facades are heavily insulated, to simulate the performance of the adjacent house, avoiding extra gains, and a ventilated façade is added to limit solar gains.

In the city of Dezhou, Shandong, China, thermal loads at summer and winter design conditions were estimated to be 16 kW for cooling and 9 kW for heating. To cover these loads, the HVAC system (Figure 3) of the prototype was developed focusing on the modularity and feasibility of the project. All the technologies applied for the systems are market-available. The cooling system

is composed of a Variable Refrigerant Volume (VRV-Daikin®) Heat Pump connected with four internal units with enhanced dehumidification capability. The heating system is composed of a 4-loop capillary heating system that is fed by the same external heat pump through a high efficiency heat exchanger. The four loops are independent, the mats are pre-casted inside the concrete of the floor in the main conditioned rooms.

There is a recycling system for the grey water and condensate from the HVAC system, which saves around half of a typical water consumption, and uses the purified water to different purposes: plants irrigation, toilet flush, sprinkler system, rain garden.

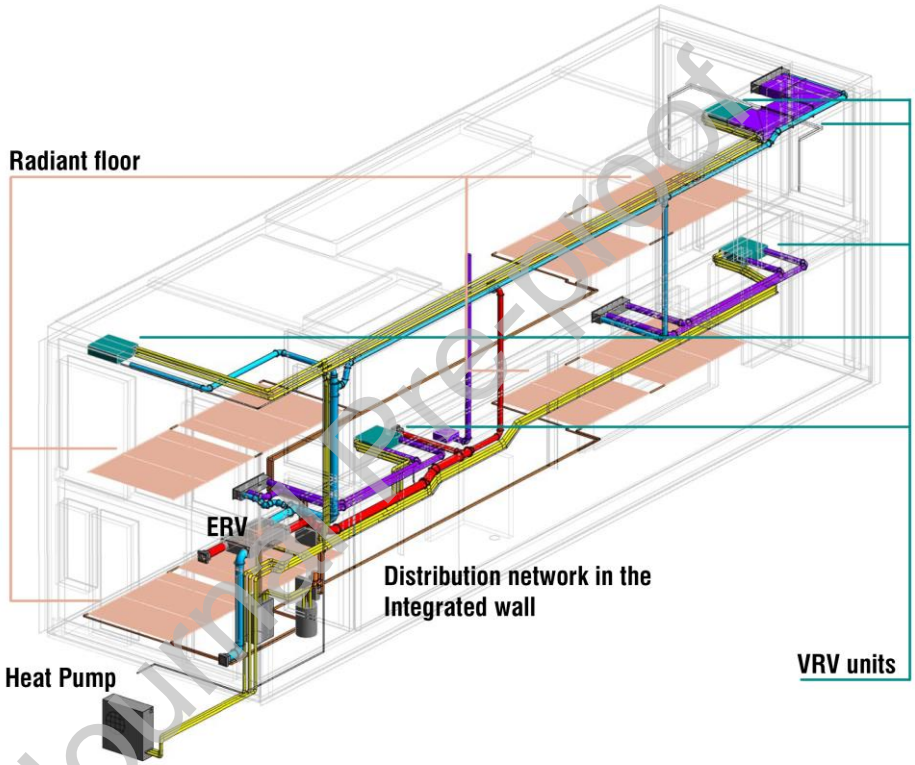

Figure 3: 3-D Schematic of the HVAC system

The ventilation system was designed to reduce the CO_2 and PM2.5 concentration in the inside air. An Energy Recovery Ventilator was designed to provide a fresh air flow of 350 m^3/h. The outdoor air is firstly filtered in a coarse filter and then in a finer one, obtaining a filtering efficiency to the PM2.5 >99%. The air then passes through a counter flow heat exchanger in which it exchanges sensible energy with the exhaust air to reduce the conditioning load on the inside. The air is sent directly inside the living belt, in the 4 conditioned rooms, while the extraction is located in the corridor of the first floor and next to the top of the aquaponic system on the second floor (this position was selected to highly reduce the amount of humidity in the

proximity of the green wall). The flow path is ensured by the normal air leakage of the internal doors without considerably increasing the pressure drops.

On the roof, 11 kW_p of high-efficiency PV panels are installed on a steel structure. The electricity generated is supposed to be used in the building and to charge the battery of an electric vehicle. There are also 6 m^2 of solar thermal panels to produce domestic hot water, combined with an electrical resistance to increase availability and temperature control.

2. Methods

2.1. Optimization-based calibrated simulation

The procedure for the calibration set-up is composed of the following steps (Figure 4):

- Measurement campaign to gather data on the weather conditions and the internal temperatures of thermal zones;
- Creation of the Building Energy Model (BEM), with implementation of the measured weather data into the model;
- Sensitivity analysis on the BEM input parameters to determine the calibration parameters;
- BEM handling to create the coupling with the optimization software;
- Iterative Optimization to calibrate the model accordingly with the progress of the construction site:
    - "free floating" calibration, which calibrates the envelope parameters based on measured and simulated indoor air temperatures when the building is running in free-floating and HVAC system is in progress of installation or is not working properly;
    - "final calibration", which considers both envelope and system parameters as it is performed after the completion of the building construction in the contest location;
- Data Post Processing leading to possibility of active intervention on the final design, construction and operation strategies of the building prototype.

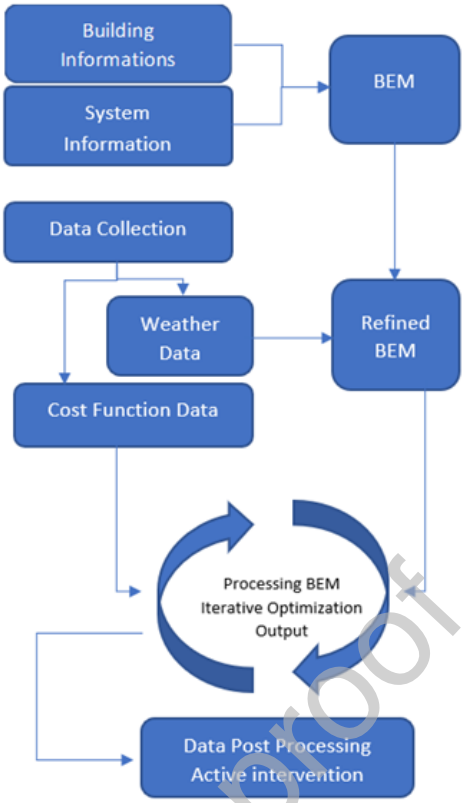

Figure 4: Optimization-based calibration framework

2.1.1. Measurements: data collection

As mentioned, a large set of measured data is necessary to calibrate a building simulation model. The measurement campaign was organized in parallel with the last phase of construction of the building.

The first dataset is related to weather data, which were collected by means of:

- Davis Vantage Pro2 weather station [22];
- Delta Ohm HD2102 Solar Flux Datalogger [23] ;
- LP Pyra02 Pyranometer [24].

The position of the sensors was set to reduce the effect of nearby building or environment and maintain the sensors safe from the building site operation [25].The weather station was placed on the north-west corner, with the wind probe at the height of 3 meter (first floor). The Pyranometer was placed on top of the workers stall to reduce the horizontal interaction with other structures and avoid any kind of shading (allowed <5° on the horizontal).

Another dataset was collected regarding internal temperatures of thermal zones, to proceed with the so-called temperature calibration [25]. The analysis of the temperature evolution can highlight the accuracy of the simulation and is easily gatherable. Measurements were organized dividing the thermometers (HOBO U23-001 [26]) according to their timestep (2 minutes- Therm.

A and 5 minutes - Therm. B). Therm. A were placed in couples in the main thermal zones, while The Therm. A, used for the actual measurements, were placed at the geometrical centre of the zone at a height of 1.5 m as shown in Figure 5. Therm. B were placed at the top of walls in the connection zones and were used to check the temperature fluctuation between zones. The location of sensors in the building thermal zones (see par. 2.1.2 and Table 1 for thermal zones details) is reported in Figure 6.

At the beginning of the prototype construction phase, which lasted a couple of weeks, the activities focused on the measurement architecture, the sensors placement and model updating with the actual prototype configuration. This led to carry out measurements for 3 days, allowing a level 4 calibration, based on short-term monitoring [16].

Figure 5: Picture of the placement of temperature sensors

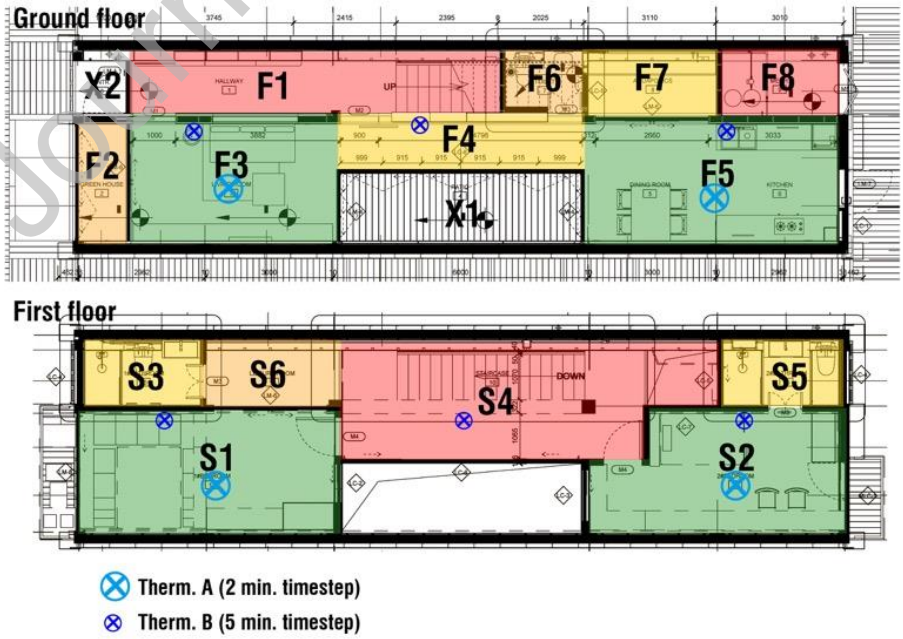

Figure 6: Plans of the building: thermal zoning and placement of temperature sensors

2.1.2. The simulation model

The simulation model was created in TRNSYS®. In order to increase the model level of detail while maintaining the calculation manageable, the overall modelling was split into the Building Model (BM), describing the building envelope behavior and the related energy needs, and the HVAC System Model (SM).

The core Type for the BM simulation is the Type-56; it allows a detailed description of the envelope and the 16 different zones (Table 1), simulated through a nodal configuration. The 4 zones reported in bold in Table 1 are directly conditioned. This detailed model zoning allows direct control of the conditioned spaces even if they are part of a bigger open space [27]: smaller thermal zones implies higher control on the ventilation flow path and higher precision on the temperature and humidity values in that particular part of the prototype. These characteristics are fundamental to reduce the averaging effect of the temperature in other zones and limit the mismatch between the simulated and measured values.

Table 1: Description of thermal zones defined in the simulation model (ref. Figure 6)

Code	Room/Zone	Vol [m^3]
F1	Hallway	20.7
F2	Greenhouse	9.6
F3	**Living Room**	**39.7**
F4	Corridor	20.3
F5	**D.R.+Kitchen**	**49.4**
F6	Bathroom 1	6.9
F7	Aquaponics	13.4
F8	Mechanical Room	10.6
S1	**Bedroom 1**	**49.3**
S2	**Bedroom 2**	**44.3**
S3	Bathroom 2	12.0
S4	Staircase	81.1
S5	Bathroom 3	12.0
S6	Leisure Room	14.6
X1	Patio	61.6
X2	Cabinet	3.0

The SM includes the cooling, the ventilation and the heating system, although the latter was switched off during the contest simulation. In addition to this, the simulation includes the management system, and graphical and numerical output.

The ventilation model considers the infiltration from openings and air flows based on pressure and temperature differences between the different zones. It was created through the coupling

between TRNSYS and CONTAM Multizone Air Flow, which also allowed simulating the chimney effect.

The Cooling system was simulated using 4 different standard split types. The part load power was defined through an equation type that determines the energy needed to reach the setpoint based on the room temperatures at each timestep.

This equation was developed from the COP table in part load provided by the producer through a polylinear regression (Figure 7). The resulting goodness-of-fit is as follows:

- R-square: 0.9964
- Adjusted R-square: 0.9961
- RMSE: 0.1329

The external unit type reads the part load as the sum of all the power used by the internal units and the outdoor temperature from the weather file and give the COP as an output to evaluate the electrical energy consumption.

The control of the system set-point temperature was modeled using the TRNSYS type 698 (Five stages room thermostat for *n* temperatures), in combination with the detailed CONTAM modelling of the convection within and between spaces. This allows modelling the fact that the cooling unit is placed at a specific location in the room and it does not add energy evenly to the space in the framework of assumptions and simplifications required by energy simulation, leading to potential differences between the indoor air temperature registered at the center of the thermal zone and the one registered in proximity of the cooling units.

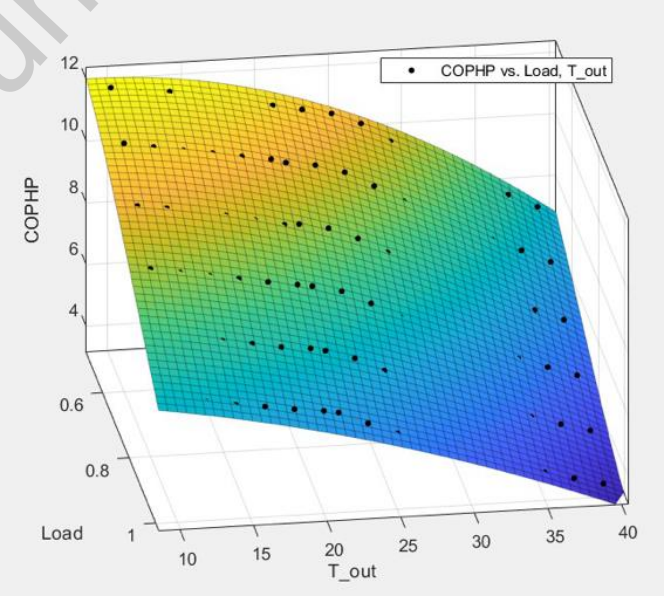

Figure 7: Model of the system COP in part load

2.1.3. Sensitivity analysis

The described modelling assumptions determine a list of 302 simulation input parameters, but only some of them can be actively used for calibration due to their source or the use done in the simulation, as highlighted by R. Enriquez at al. [28]. Moreover, the number of calibration parameters should be limited to ensure acceptable computational time. A first user selection can be performed [29], but then it is necessary to ensure that the selected parameters are those having the highest impact on the simulation outcome. This can be done through sensitivity analysis.

Several Sensitivity Analysis methods could be applied to a model giving different information about the input parameters [30]. The Morris method was selected as a compromise between the so-called local (high level of information about inputs) and global methods (no information about inputs) [31]. This procedure shares some characteristics from both local and global methods [32], of which the advantages are as follows:

- The influence sorting of the parameters is provided;
- The method does not depend on properties and does not require linearity assumption (difficult to make using building energy models);
- The hyperspace can be explored evenly without defining parameters' probability density functions in advance;
- Results can be graphically interpreted;
- The computational time is limited;
- Its implementation is relatively easy.

The Morris Method works using "trajectories": from a first step in the hypercube of possible values the coordinates move variating only one parameter at each step. It relies on the evaluation of a Sensitivity Index several times for every parameter. Such Index is called Elementary Effect and is defined as

$$EE_i\left(\underline{X}^j\right) = \frac{Y\left(X_1^j,\dots,X_{i-1}^j,X_i^j+\Delta,X_{i-1}^j,\dots,X_k^j\right)-Y\left(\underline{X}^j\right)}{\Delta} \qquad (1)$$

where *Xi* is one of the *k* parameters composing a system and *Y* represents the system's output before and after the variation of the i^{th} parameter of the quantity Δ. Once the Elementary effect is computed for each of the *r* trajectories *j*, the mean value μ_i and the standard deviation σ_i are evaluated as follows (Equations (2) and (3)), to allow the sorting of the parameters.

$$\mu_i = \frac{\Sigma_{j=1}^{r} EE_i\left(\underline{X}^j\right)}{r} \qquad (2)$$

$$\sigma_i = \sqrt{\frac{\Sigma_{j=1}^{r}\left[EE_i\left(\underline{X}^j\right)-\mu_i\right]^2}{r}} \qquad (3)$$

Since the Elementary Effect could assume negative values, to avoid cancellation errors it is good practice to also evaluate the absolute mean value of the Elementary Effect as follows (Equation (4)).

$$\mu_i^* = \frac{\Sigma_{j=1}^{r} |EE_i(\underline{X}^j)|}{r} \qquad (4)$$

The resulting value of μ_i^* indicates the overall importance of the parameter *i* on the simulation output, while σ_i indicates non-linear effects and interactions between parameters. It has to be remarked that those are qualitative measures, providing indications on how to rank parameters in order of importance, but they do not exactly quantify the influence of each parameter on the model. In general, parameters related to high values of μ_i^* and σ_i should be selected as the most influential.

The Morris method was implemented through a MATLAB code after the Optimized Latin Hypercube Sampling was performed, based on the so-called Campolongo's procedure [33], to obtain a set of exhaustive trajectories to explore the solution space and limit the risk of leaving unexplored large parts of the parameter space. This led to determine 10 different trajectories.

The parameters were set as variable in the TRNSYS simulation input files with a batch file calling a function to write the value of the parameter accordingly to the trajectory at that step. The list of 29 selected input parameters and the range for their variation is reported in Table 2.

In order to ensure their weight is the same within the analysis, 4 steps were defined for each variation range. When the reported unit is "%", it means that the variation of that parameter is based on a percentage value that modifies the initial design values of parameters.

Table 2: Input parameters for sensitivity analysis

#	Parameter	Min	Max	Unit
1	ERV Sensible Effectiveness	-0.1	0.1	%
2	Internal Convective Heat Transfer Coefficient	5	9	kJ/hm^{2}K
3	External Convective Heat Transfer Coefficient	55	75	kJ/hm^{2}K
4	Internal Convective Heat Transfer Coefficient_W	5	9	kJ/hm^{2}K
5	External Convective Heat Transfer Coefficient_W	55	75	kJ/hm^{2}K
6	Infiltration flow rate F3	-0.1	0.1	%
7	Infiltration flow rate F5	-0.1	0.1	%
8	Infiltration flow rate S1	-0.1	0.1	%
9	Infiltration flow rate S2	-0.1	0.1	%
10	Air coupling zones F1-S4	-0.1	0.1	%
11	Air coupling zones F7-S4	-0.1	0.1	%
12	Shading Factor Horizontal	0	0.1	-

13	Air flow natural ventil.	0	700	m^3/h
14	U-Value Frame Windows type #1	-0.1	0.1	%
15	Area frame/glass Windows type #1	0.1	0.2	%
16	U-Value Frame Windows type #2	-0.1	0.1	%
17	Area frame/glass Windows type #2	0.1	0.2	%
18	U-Value Frame Windows type #3	-0.1	0.1	%
19	Area frame/glass Windows type #3	0.1	0.2	%
20	Zones Capacitance F3/Volume	35	55	kJ/K
21	Zones Capacitance F5/Volume	50	70	kJ/K
22	Zones Capacitance S1/Volume	50	70	kJ/K
23	Zones Capacitance S2/Volume	45	60	kJ/K
24	Phenolic Conductivity	-0.05	0.05	%
25	VIP Thermal resistance	-0.05	0.05	%
26	Approx. average ground surface temp.	293	303	K
27	Absorbance Frame Windows type #1	-0.1	0.1	%
28	Absorbance Frame Windows type #2	-0.1	0.1	%
29	Absorbance Frame Windows type #3	-0.1	0.1	%

2.1.4. Simulation-based optimization for calibration

As mentioned, the proposed approach involves the coupling of a Building Energy Modelling Software, TRNSYS®, with an Optimization program, GenOpt®. To perform such optimization-based calibration, an optimization cost function should be set, based on the difference between the measured and the simulated data set. In this work, the optimization objective function was set according to the standards for considering a calibration validated; this was done in order to achieve within the same operation both the calibration and its validation. The standard used for reference is the ASHRAE Guideline 14 (ASHRAE, 2002). The validation of the calibration is based mainly on two statistical indices (S - simulated data; M - measured data):

- Normalized Mean Bias Error (NMBE)

$$NMBE(\%) = \frac{\Sigma_{Period}(S-M)_{interval}}{\Sigma_{Period}M_{interval}} \cdot 100\% \quad (5)$$

- Coefficient of Variation of the Root Mean Square Error (Cv(RMSE))

$$Cv(RMSE_{Period}) = \frac{RMSE_{Period}}{A_{Period}} \cdot 100 \quad (6)$$

$$RMSE_{Period} = \sqrt{\frac{\Sigma(S-M)^2_{interval}}{N_{interval}}} \quad (7)$$

$$A_{period} = \frac{\Sigma_{Period} M_{interval}}{N_{intervl}} \quad (8)$$

Therefore, the cost function that the optimization process has to minimize can be expressed as follows

$$CF = NMBE \cdot 0.5 + Cv(RMSE) \cdot 0.5 \quad (9)$$

where the same statistical weight is assigned to both the NMBE and the Cv(RMSE) and constraints are set for both NMBE and Cv(RMSE)so that they are below the threshold limits reported in the ASHRAE Guidelines (NMBE: ±10%; Cv(RMSE): 30%).

For the optimization in GenOpt, a hybrid global optimization algorithm was selected [34]. This algorithm starts with a Particle Swarm Optimization (PSO) on a mesh, for a number of generations n_G defined by the user. Then, it initializes the Generalized Pattern Search (GPS) algorithm for the continuous independent variables, while discrete variables are fixed at the value of the particle with the lowest cost function value. Thus, the hybrid algorithm combines the global features of the PSO algorithm with the provable convergence properties of the GPS algorithm, thus ensuring higher accuracy while limiting the risk of being attracted by local minima.

Being the algorithm already pre-loaded in the GenOpt scripts, it only needs some simple commands to perform the optimization. It is required to write the GenOpt configuration file, containing indication about the simulation program to call, and the command file, where the optimization parameters are defined and the and algorithm settings are reported.

Moreover, the simulation should be prepared to ensure that the TRNSYS input file is ready to be called iteratively by GenOpt and evaluate the cost function according to the calibration objectives.

First of all, a user-defined weather file was created based on the data collected from the weather station. The TRNSYS *Type 109-Userdefined* was used to input the so-created weather file to the model.

Then the temperatures measured in the zones have to be read by the simulation to evaluate the deviation of the calculated data from the real ones. The format used is the simple Type9a: this type allows to create a simple tab with interpolating features and user-defined time interval.

Then, at each simulation run, a MATLAB script called within the TRNSYS simulation allows evaluating the cost function on hourly-averaged values provided by a TRNSYS output file. The script handles the temperatures, measured and simulated ones, of all the 4 different zones separately, and proceeds with the calculation of the cost function using the worst condition (the data set that are on average on the biggest distance).

As a last step, the coupling between TRNSYS and GenOpt should be finalized by editing the TRNSYS input files. The editing entails creating two template files where GenOpt is able to write different values of optimization parameters driven by the algorithm, thus creating different simulation input files at each iteration.

2.2. Combined design and operation ZEB optimization

The second step of the work, related to the combined design and operation optimization of the building, relies on the simulation-based optimization framework that was previously described, with some adjustments. As shown in Figure 8, the complete framework relies on the use of TRNSYS, supported by CONTAM, to perform detailed energy simulations using the previously calibrated building model. The TMY weather file referring to Raoyan, a city close to the contest location, was selected for simulations carried out in this step. MATLAB was used to manage simulation outputs and calculate the new objective function, while GenOpt was used to set up optimization variables and drive the optimization process.

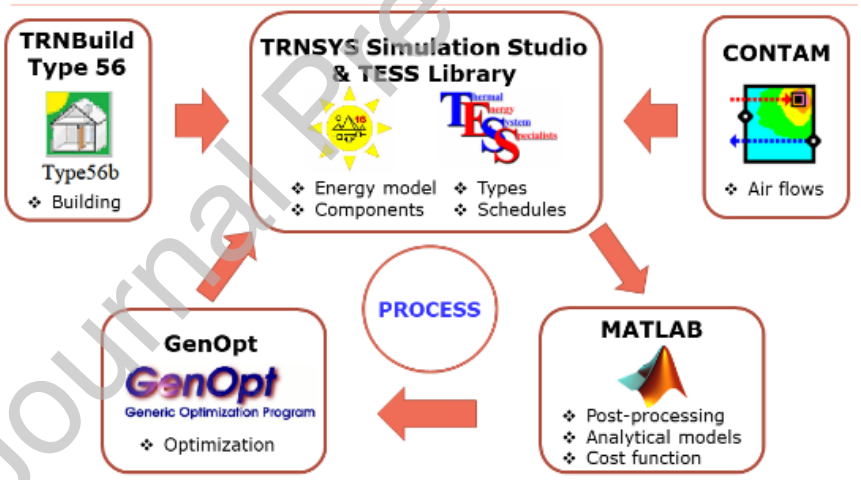

Figure 8: Optimization framework and used tools

2.2.1. The contest score optimization objective

As mentioned, the objective of the optimization study is to maximize the contest score. For this purpose, this objective has to be translated into a dedicated cost function that is computed by the involved tools. Therefore, the set of objective criteria related to zone variables that can be monitored, simulated and therefore optimized to maximize their contribution to the final score are included in the so-created objective function (Equation 10). Non-objective criteria have been excluded from the computation as they are subject to the jury's judgements and cannot be simulated nor optimized.

The formulation of the objective function is as follows:

$$P_{TOT} = \sum_{i=1}^{\tau}(P_{T,i} + P_{RH,i} + P_{CO2,i} + P_{PM,i}) + P_{EB} \quad (10)$$

where

- i is the time-step for score calculation, which the Solar Decathlon rules set to 744 set to 15 minutes for the evaluated variables included in this function;
- τ is the total number of evaluated time-steps in the contest period, which the Solar Decathlon rules set to 744 for the evaluated variables included in this function - it has to be noted that these time-steps may not be consecutive and occur either during the day or the night of different contest days;
- $P_{T,i}$ are the points related to the indoor air temperature T_i [°C], calculated at the time-step i according to Equation (11) - the maximum achievable value for $P_{T,i}$ over τ is 40 points;

$$P_{T,i} = \begin{cases} \frac{40}{\tau} & 22 \le T_i \le 25 \\ \frac{40}{\tau} \cdot \frac{T_i - 19}{22 - 19} & 19 \le T_i < 22 \\ \frac{40}{\tau} \cdot \frac{T_i - 28}{25 - 28} & 25 < T_i < 28 \\ 0 & in\ all\ other\ cases \end{cases} \quad (11)$$

- $P_{RH,i}$ are the points related to the indoor relative humidity RH_i [%], calculated at the time-step i according to Equation (12) - the maximum achievable value for $P_{RH,i}$ over τ is 20 points;

$$P_{RH,i} = \begin{cases} \frac{20}{\tau} & 0\,\% \le RH_i \le 60\,\% \\ \frac{20}{\tau} \cdot \frac{RH_i - 70}{60 - 70} & 60\% < RH_i \le 70\% \\ 0 & in\ all\ other\ cases \end{cases} \quad (12)$$

- $P_{CO2,i}$ are the points related to the CO2 level [ppm], calculated at the time-step i according to Equation (13) - the maximum achievable value for $P_{CO2,i}$ over τ is 20 points;

- $$P_{CO2,i} = \begin{cases} \frac{20}{\tau} & 0 \le CO2_i \le 1000 \\ \frac{20}{\tau} \cdot \frac{CO2_i - 1000}{2000 - 1000} & 1000 < CO2_i \le 2000 \\ 0 & in\ all\ other\ cases \end{cases} \quad (13)$$

- $P_{PM2.5,i}$ are the points related to the PM2.5 level [µg/m^3], calculated at the time-step I according to Equation (14) - the maximum achievable value for $P_{PM2.5,i}$ over τ is 20 points;

$$P_{PM2.5,i} = \begin{cases} \frac{20}{\tau} & 0 \le PM2.5_i \le 35 \\ \frac{20}{\tau} \cdot \frac{PM2.5_i - 35}{75 - 35} & 35 < PM2.5_i \le 75 \\ 0 & in\ all\ other\ cases \end{cases} \quad (14)$$

- P_{EB} are the points related to the energy balance EB [kWh/m^2], calculated as the difference between production and consumption over the entire contest period, according to Equation (15) - the maximum achievable value for P_{EB} is 80 points.

$$P_{EB} = \begin{cases} 80 & EB \ge 0 \\ 80 \cdot \frac{EB}{50} & -50 \le EB < 0 \\ 0 & in\ all\ other\ cases \end{cases} \quad (15)$$

The above-listed criteria are related to a maximum of 180 points out of 1000. Such points may be decisive for final ranking, considering that usually the Solar Decathlon teams compete for the first positions with tiny differences of points.

The cost function was implemented in MATLAB and linked to the input variables simulated in the TRNSYS model, considering the complex schedules of the contest. In fact, the formulation of this objective function accurately reflects the score calculation that was planned for each day of the contest period, having different schedules for the monitoring periods (in which the above listed environmental parameters are measured and evaluated) and for the tasks performing periods (tasks include domestic energy-consuming activities like doing the laundry, preparing meals, or inviting friends for a party). The energy balance is calculated at the end of the simulated contest period, to reproduce the score calculation planned for the contest.

2.2.2. Optimization variables

Once the optimization objective and the energy model were defined, the design variables impacting the created cost function were identified. Twenty-four variables were selected, some related to the building envelope and others related to the system design and operation, as reported in Table 3.

The set of optimization variables represents the set of design variables that could be controlled by the simulation model and could be checked and optimized during the construction and the pre-contest test phases. Their selection was performed according to real feasibility criteria, but it has to be noted that other measures related to other design variables could potentially lead to better performance in terms of energy saving and improved comfort.

The selected design-related variables refer to the tilt angle of the PV panel and the thickness of the massive and light layers of envelope (OSB and phenolic insulation). Some of them are set for different orientations, to evaluate their influence on the performance and thus on the contest score. The operation-related variables refer to the cooling setpoint, the ERV operation schedules, the shading fraction and the related time schedules.

The range of variation and the step length of the selected set of optimization variables is reported in Table 3. They were set as discrete variables in order to reflect their variation possibilities in the reality. This was done according to market availability criteria for design-related variables (e.g. the available OSB panels are 12 mm thick), while operation-related variables were set according to feasibility and easiness-of-use criteria (e.g. a fraction of 0.62 for the shading devices is not smart because not practically useful).

This lead to define a search space composed of $3.85 \bullet 10^{16}$ possible combinations of design/operation options.

Table 3: Settings of optimization variables.

Name	Description	Unit	Min	Max	Step length
T_VRV	Setpoint Temperature	°C	20	25	1
ERV_on1	ERV turn on time day 1	hour	16	18	0.5
ERV_on2	ERV turn on time day 2	hour	19.5	21.5	0.5
ERV_off1	ERV turn off time day 1	hour	19.5	21.5	0.5
ERV_off2	ERV turn off time day 2	hour	22	24	0.5
PV_angle	Array Slope	°	0	25	5
Sh_N	Shading North	Fraction	0	1	0.5

Sh_S	Shading South	Fraction	0	1	0.5
Sh_H	Shading Horizontal	Fraction	0	1	0.5
Sh_N_on	Shading Time ON North	hour	7	12	1
Sh_S_on	Shading Time ON South	hour	7	12	1
Sh_H_on	Shading Time ON Horizontal	hour	7	12	1
Sh_N_off	Shading Time OFF North	hour	17	22	1
Sh_S_off	Shading Time OFF South	hour	17	22	1
Sh_H_off	Shading Time OFF Horizontal	hour	17	22	1
OSB_N	OSB thickness, North wall	mm	0.012	0.036	0.012
OSB_S	OSB thickness, South wall	mm	0.012	0.036	0.012
OSB_Roof	OSB thickness, Roof	mm	0.012	0.036	0.012
OSB	OSB thickness, Other surfaces	mm	0.012	0.036	0.012
INS_N	Phenolic Insulation thickness, North	mm	0.10	0.24	0.02
INS_S	Phenolic Insulation thickness, South	mm	0.10	0.24	0.02
INS_H	Phenolic Insulation thickness, Roof	mm	0.10	0.24	0.02
INS	Phenolic Insulation thickness, Other	mm	0.10	0.24	0.02
INS_int	Phenolic Insulation thickness,Int. Walls	mm	0.10	0.24	0.02

2.2.3. Optimization settings and runs

As described, the optimization problem is characterized by discrete variables. The Particle Swarm Optimization (PSO)[35][36] was selected because it does not depend on the nature of the objective function, it limits the risk of getting stuck in local optima and it leads to a great number of cost function evaluations, for a deep exploration of the search space [37]. In particular, the binary PSO implementation of the generic optimization program GenOpt® was used, because of its ability in dealing with discrete variables and its demonstrated ability to deal with building-related problems [38][39].

The coupling between TRNSYS, GenOpt and MATLAB was performed similarly to what is described in paragraph 2.1.4 for optimization-based calibration. A new MATLAB script was created to handle the simulation outputs in relation to the points gained for the contest purpose at each iteration of the optimization process.

The time required for one iteration (corresponding to one simulation run) is around two minutes, in a computer equipped with a processor Intel Core I7-6700HQ (2.6 GHz) and 8 GB RAM. The time for the optimization, obviously, grows as the number of generations and particles grows. Therefore, in order to limit the computation time, it is very important to determine how

many iterations are required to reach the optimum, that is the maximization of the cost function, and how much it varies according to the number of iterations and the other algorithm settings.

Therefore, several optimization runs were performed to check the efficiency of the algorithm and the effectiveness of the tool and adjust their settings. In particular, according to the approach followed in [38], different numbers of iterations were tested, varying the number of particles, the number of generations, and also different combinations of the PSO algorithm social and cognitive accelerations. It has to be noted that, because the global optimum is known (it corresponds to the 180 points for the contest score), this constitutes also a test for the ability of PSO algorithm in dealing with building optimization problems.

3. Results and discussion

3.1. Model calibration

3.1.1. Results of the sensitivity analysis

The sensitivity analysis was launched with the aim of creating two sets of parameters to be used for the two different steps of calibration: one regarding the envelope calibrated simulation, here called "free floating" calibration, and the other for the final calibration including also the system performance. The resulting set of selected parameters, in relation with the two indices μ and σ (indicating mean and standard deviation of elementary effects – Eq.(1) over trajectories) are shown in Figure 9. The orange round-shaped points represent the set of 7 parameters used for the free-floating calibration, violet square-shaped represent the set of 10 parameters used for final calibration, while the red cross-shaped points are the discarded parameters. The selected parameters are also reported in Table 4. Refer to Table 2 for numbering and description of parameters.

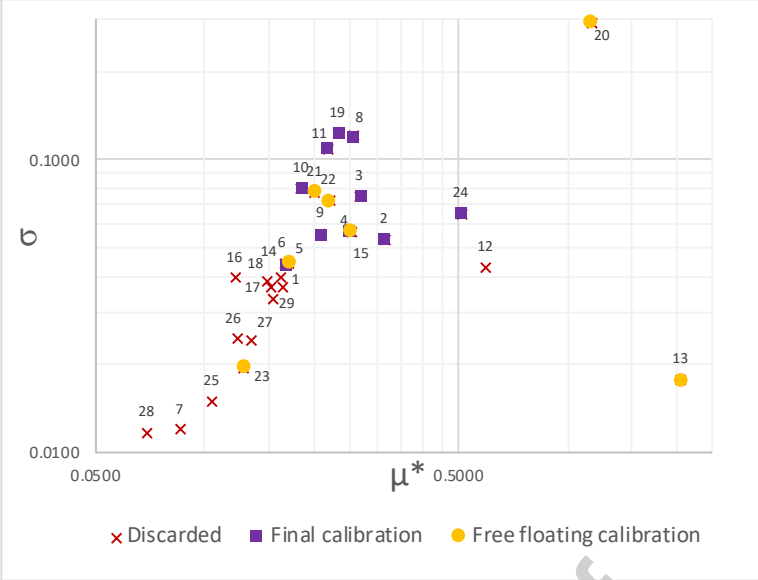

Figure 9: Parameter selection from sensitivity analysis

Table 4: Set of parameters selected for calibration

Free Floating Calibration			**Final Calibration**		
#	μ*[kWh]	σ[kWh]	#	μ*[kWh]	σ[kWh]
13	2.0583	0.0177	6	0.1672	0.0441
15	0.2539	0.0568	19	0.2335	0.1240
21	0.2020	0.0773	8	0.2568	0.1211
22	0.2207	0.0726	24	0.5109	0.0652
20	1.1619	0.2946	3	0.2683	0.0752
23	0.1288	0.0196	4	0.2509	0.0576
5	0.1711	0.0444	2	0.3137	0.0534
			11	0.2181	0.1089
			9	0.2095	0.0557
			10	0.1851	0.0803

3.1.2. Free Floating Calibration

For the free-floating calibration, the simulation was rearranged to speed up the runs removing the components related to systems that, due to the building site operation, were not used. The resulting reduced simulation maintains the infiltration handlers, the air coupling simulation in CONTAM. Within the optimization process, the simulation was iteratively launched for a 72 h range with a 1 minute timestep. The related weather file was defined, based on the collected data from the weather station.

Here are reported the results related to the free-floating calibration of the model that was performed during the finalization of the first prototype construction, happened in May 2019 in Guangzhou. The minimization of the cost function (Equation (9)) during the optimization process is shown in Figure 10, where all the evaluated solutions are ordered with respect to the calibration cost function value.

The resulting optimal set of parameter values is reported in Table 5, while the goodness of fit according to the ASHRAE thresholds is reported in Table 6. As shown, the model resulted to be well calibrated.

The graphs in Figure 11 report the simulated indoor temperature (red) of the worst-performing zone (F3 – living room) with respect to the measurements (black) and the outdoor temperature profile (grey) in a sample day. The first graph in Fig. 11 shows the pre-calibration conditions. In the second graph, reporting the conditions after the free-floating calibration, it is shown that the deviation during daytime is almost totally reduced and differences in the behavior during nigh time appear just in presence of sudden change in outdoor conditions.

This calibrated model was used to start running optimizations for supporting the finalization of design strategies to maximize the contest score, before the beginning of the final prototype construction in the contest location.

Table 5: Optimized parameters values-free floating calibration

#	Parameter	Description	Value	Unit
13	AC_od	Air Flow Natural Ventilation	25	m^3/h
15	Rat_fr_fac	Ratio Frame/Glass	0.2	%
20	Cap_f3	Capacitance of thermal zone/Volume	51	kJ/K
21	Cap_f5		69	
22	Cap_s1		69	
23	Cap_s2		58	
5	HW_out	External Convective Heat Transfer Coefficient_Windows	59	kJ/hm^2K

Table 6: Result validation – free floating calibration

	Value	Threshold	Validated
NMBE (%)	+4.27	±10	x
Cv(RMSE)	+4.88	30	x

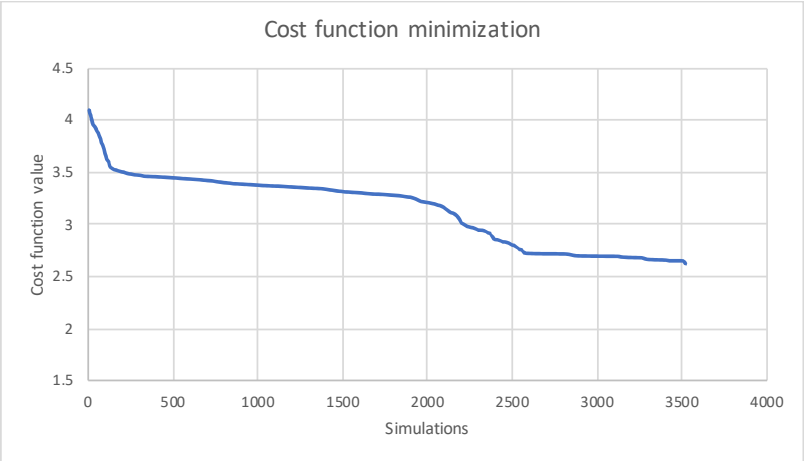

Figure 10: Cost function minimization

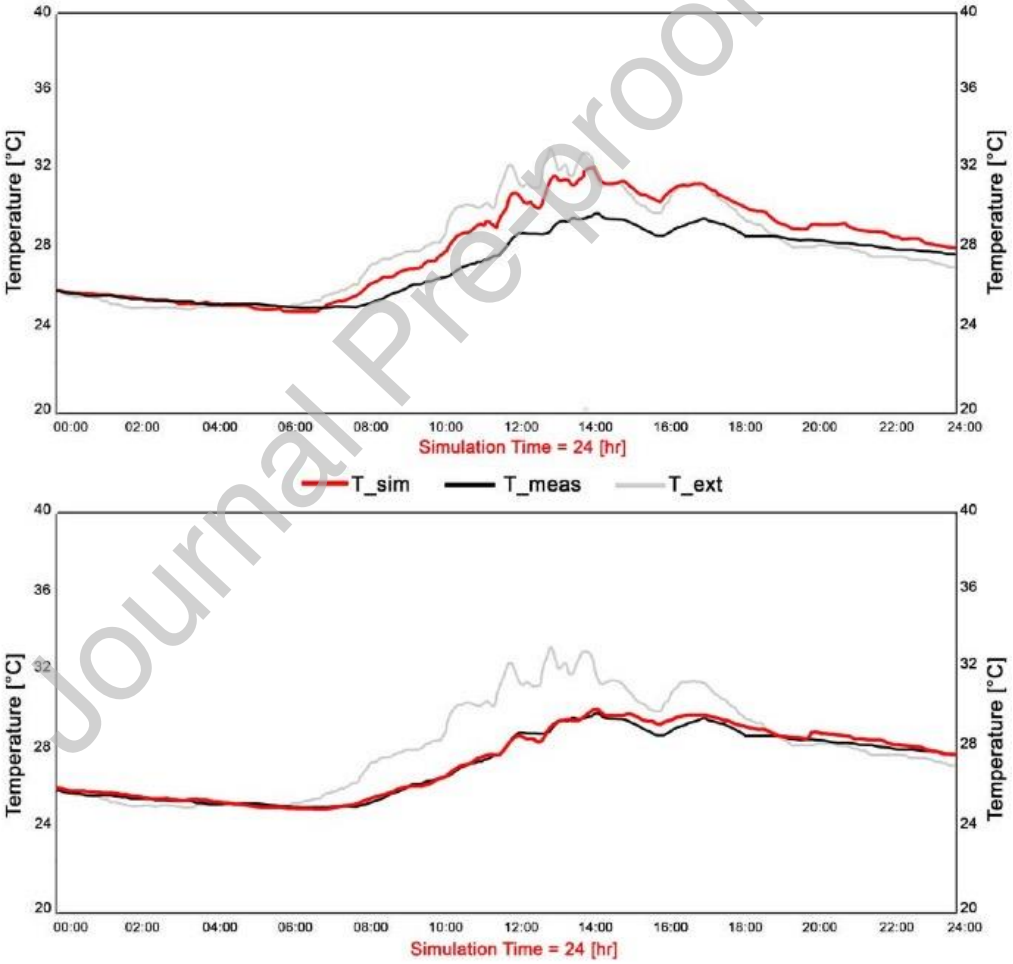

Figure 11: F3 (living room) zone temperatures pre and post calibration in a sample day

3.1.3. Final Calibration

The final construction of the prototype in the building location (Dezhou) was performed in strict relation with simulation. Based on the previously calibrated model, the purpose of the final calibration was to provide a reliable simulation model of the entire building (envelope and systems) to support the definition of the last design and operational strategies before the competition.

Figure 12 refers to the comparison between simulations (pre-calibration in dotted red, post-calibration in red) and measurements (black) performed in the pre-competition days, after the second building construction. At that time the HVAC wasn't working properly, and the HVAC testing was running during the night (this is the reason why the data collected at night were not considered). Therefore, the dataset was useful to assess the "free-floating" model reliability after the second building construction, and the fact that the calibrated simulation follows the measurement profile when the HVAC system is turned off testifies the goodness of the previously performed calibration of the building envelope model.

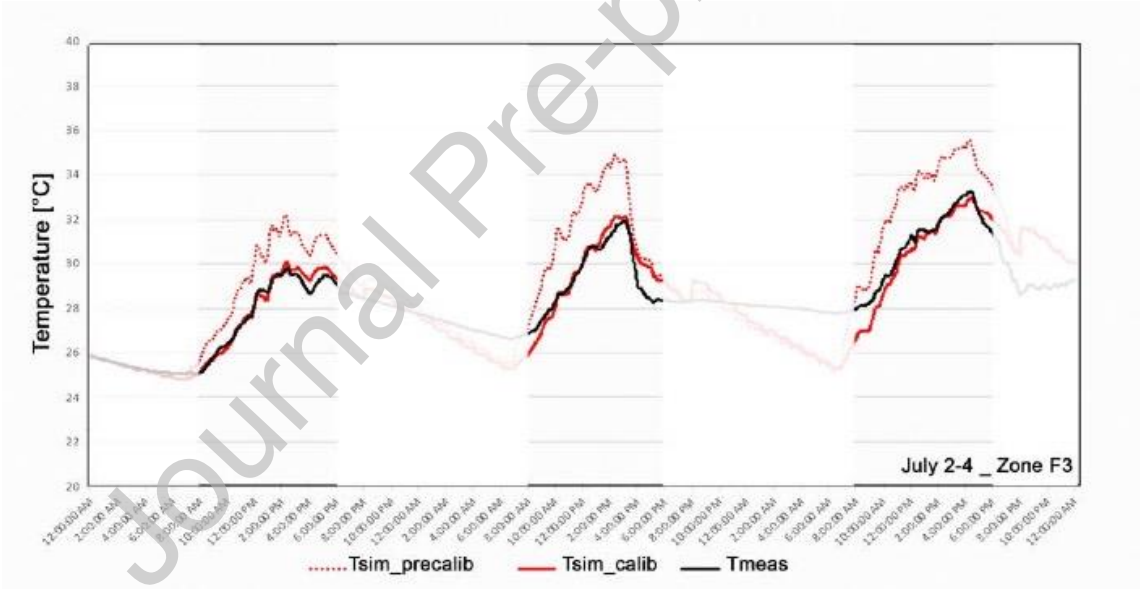

Figure 12: Measured versus simulated data during contest preparation in zone F3 (living room)

For the purpose of final calibration, due to the building site's operational status, it was possible to collect usable data only in short night time periods and proceed with a daily-based trial and error calibration to further adjust the performance of the previously optimization-based calibrated model. The fact that the most influencing parameters had already been identified through the performed sensitivity analysis facilitated the process of manually varying the values of parameters to match the behavior of the systems.

Table 7 reports the comparison between the measured and simulated data on hourly basis for indoor temperatures in the four monitored thermal zones in the last pre-competition night. Except

for the first hour, where measurements were affected by unexpected occupation in the building, the deviation between simulated and calibrated temperatures is in the range ±1 and the reported calibration indexes demonstrates that a good level of calibration was reached and that simulation could be used for short term planning during the competition.

In fact, further than leading to the final optimization runs for maximizing the contest score, with the aim of providing a benchmark on the operational mode to be maintained in the building throughout the competition (see section 3.2), the calibrated simulation became a predictive tool with a 5-8 hours timespan. Before the start of each competition monitoring period (usually occurring at night in the range 6 PM-8AM), a simulation with the expected fluctuation in the temperature was launched to validate the planned operational strategies.

Table 7: Final calibration dataset and validation

Time	***T F3 Simul.***	***T F3 Meas.***	***T F5 Simul.***	***T F5 Meas.***	***T S1 Simul.***	***T S1 Meas.***	***T S2 Simul.***	***T S2 Meas.***
18:00	22.97	24.46	23.77	27.78	23.23	28.96	23.47	25.96
19:00	23.07	23.51	23.21	26.20	23.22	27.53	23.16	24.50
20:00	24.73	23.28	24.13	25.31	23.42	26.55	23.67	23.54
21:00	24.78	23.04	24.19	24.82	23.45	24.30	23.66	23.45
22:00	25.18	22.89	25.13	24.50	24.43	23.87	24.69	23.58
23:00	24.39	24.16	24.11	24.57	23.90	23.33	24.45	23.65
0:00	24.78	23.66	24.78	24.52	24.70	23.31	24.87	23.62
1:00	24.74	23.28	24.83	24.34	24.75	23.26	24.19	23.40
2:00	24.49	23.69	24.58	24.33	24.56	23.45	24.47	23.50
3:00	24.31	23.93	24.47	24.43	24.50	23.59	24.43	23.64
4:00	23.99	23.84	24.10	24.31	24.13	23.51	24.10	23.46
5:00	23.81	24.38	23.97	24.38	24.03	23.67	24.04	23.66
6:00	24.16	23.84	24.07	24.30	23.68	23.68	24.06	23.63
7:00	23.02	23.71	23.89	24.24	22.88	23.72	23.96	23.66
NMBE (threshold: ±10)	3.96		3.48		6.39		3.49	
Cv(RMSE) (threshold: 30)	4.78		5.7		9.13		4.27	
Calibrated?	Yes		Yes		Yes		Yes	

3.2. Design and operational optimization

The diagrams in Figures 13 and 14 reports the obtained contest points (out of 180) in different optimization runs, performed at different stages of the process after each new model calibration. In particular, Figure 13 reports the starting point (initial design and operation settings) and the percentage improvement of the score after optimization runs, which ranges between 7% and 9%.

The starting score with the project data is 162.43. Each optimization shows an improvement of the solution, the maximum is around the value of 176.50 points.

In the final contest score optimization run, the maximum achieved is equal to 176.94. Because a lot of combinations of design variables leading to similar high scores were found, the last cycle of optimization runs was performed with algorithm settings tailored for a better exploration of the space of solutions. Therefore, the number of particles was increased up to 60, and the number of generations up to 30, allowing 1920 iterations. As shown in Figure 14, the last generations are reaching higher scores, up to the maximum of 176.94 points out of 180. The points related to the different categories composing the final contest score in the initial and the optimal solutions are reported in Figure 15. As shown, with respect to the initial design solution (INI), the optimization leads to improve the points related to the temperature (+6 points in the optimal solutions) and the relative humidity (+9 points in the optimal solution) parameters.

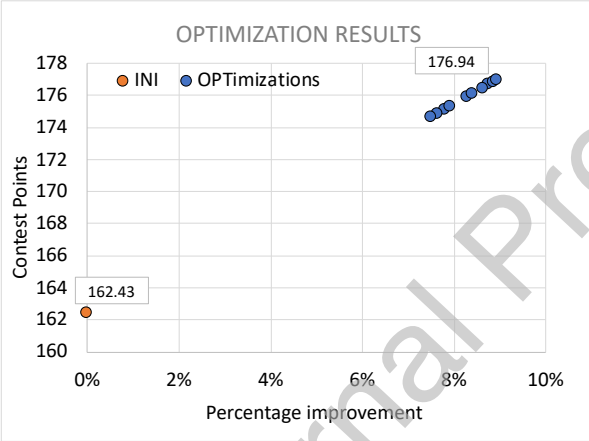

Figure 13: Contest score maximized after optimization.

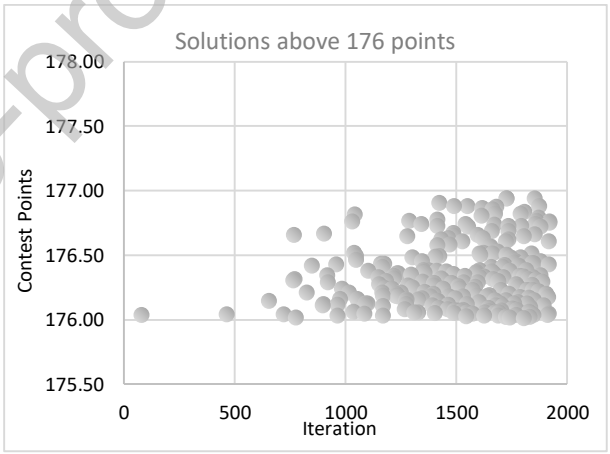

Figure 14: Solutions above 176 points.

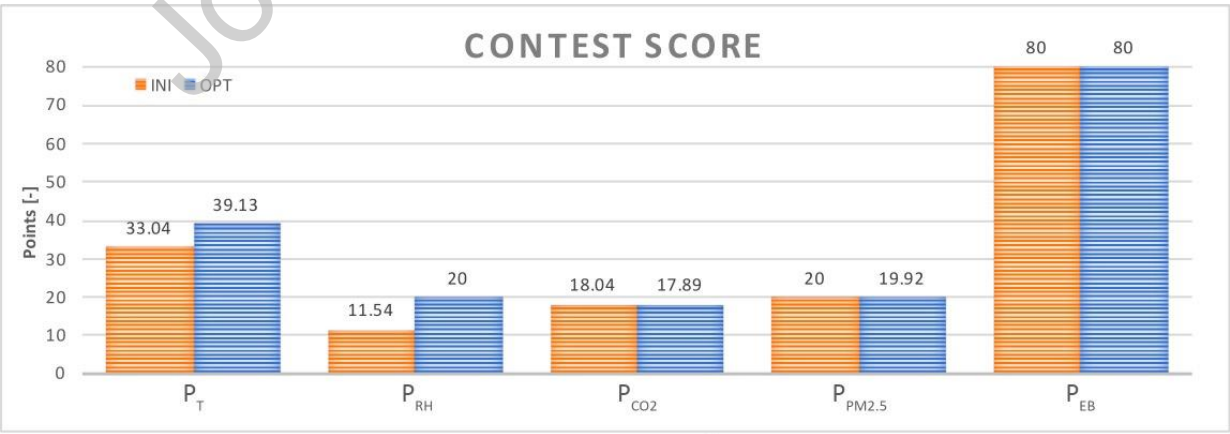

Figure 15: Splitting the contest score in the initial (INI) and optimal (OPT) solutions.

The detailed analysis of the score related to the temperature (P_T, calculated according to equation 11) and relative humidity (P_{RH}, calculated according to equation 12) is provided in

Figure 16. In particular, the relative frequency of occurrence of the different values in each time-step within the contest period is reported along with the score functions (expressed in equations 11 and 12).

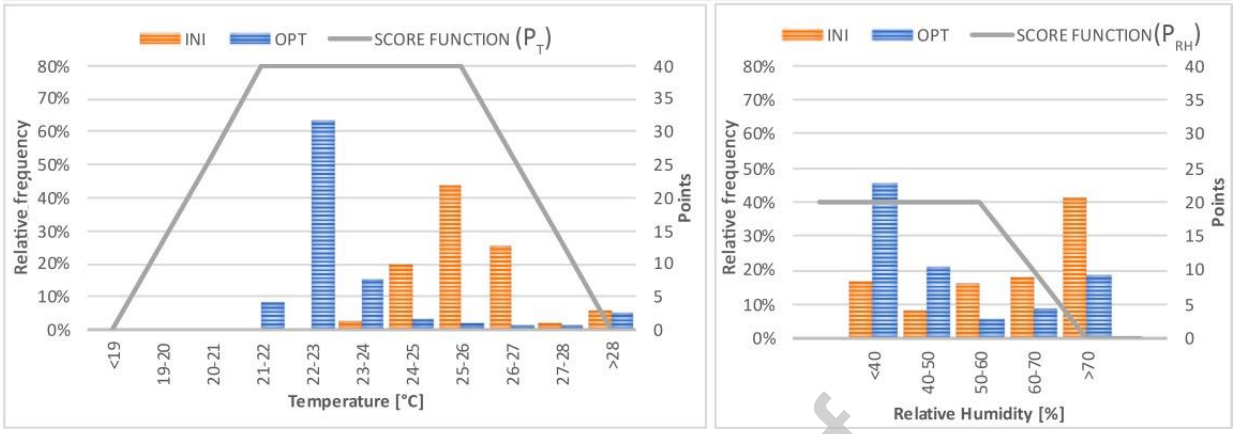

Figure 16: Relative frequency of the temperature and relative humidity values within the entire contest period in the initial and the final optimization solution.

The optimal set of parameter values, related to the maximized context score, are reported in Table 8. They were defined based on the most frequent values obtained in the neighborhood of the optimum (the set of solutions obtaining score above 176 points).

Table 8: Initial and optimal values of optimization variables.

Name	**Unit**	**Initial value**	**Optimal value**
T_VRV	°C	24	21
ERV_on1	hour	17:00	16:30
ERV_on2	hour	20:30	19:30
ERV_off1	hour	20:30	19:30
ERV_off2	hour	23:00	22:00
PV_angle	°	2	25
Sh_N	Fraction	0	0
Sh_S	Fraction	0	0.5
Sh_H	Fraction	0	0.5
Sh_N_on	hour	11:00	12:00
Sh_S_on	hour	11:00	12:00
Sh_H_on	hour	11:00	7:00
Sh_N_off	hour	19:00	20:00
Sh_S_off	hour	19:00	19:00
Sh_H_off	hour	19:00	22:00
OSB_N	mm	0.012	0.036
OSB_S	mm	0.012	0.036
OSB_Roof	mm	0.012	0.036

OSB	mm	0.012	0.024
INS_N	mm	0.20	0.12
INS_S	mm	0.20	0.12
INS_H	mm	0.20	0.14
INS	mm	0.20	0.10
INS_int	mm	0.12	0.18

As shown in Table 8, the optimization led to modify almost all the involved design and operation variables. Such modifications can be summarized and discussed as follows:

- In order to ensure high air quality score, ERV had to be turned on earlier than expected. However, to limit energy consumptions while maintaining high scores in other categories, the operation time range should be reduced by anticipating the turning off hour;
- The temperature setpoint of the VRV had to be set to 21°C, because the solar radiation and the heat stored during the day contributed to the fast rise of internal temperature;
- PV panels' tilt angle had to be higher to increase the theoretical production of the given PV area. However, tilted panels on a flat roof required a certain space between them to avoid mutual shadings, leading to reduce the available roof area;
- As expected, the shadings on the north façade do not affect the overall performance, however shadings on the other orientations (south and horizontal), had to be used at half of their capability for a larger time range than expected;
- A higher mass had to be put in the opaque envelope, as expressed through higher OSB thickness in all related variables, while insulation had to be reduced.

It has to be noted that, despite the initial purposes, there was no time to implement the resulting optimal design of the opaque envelope, due to delays in the construction phase. However, this is not so problematic in the north and south façades, because of the little areas of the opaque walls and the limited impact of such measures in the final results. This becomes important for controlling the solar radiation on the opaque roof, which is connected to the optimization outcomes related to shadings. With this in mind, the resulting optimal strategies related to shadings were carefully implemented, with the model providing an objective feedback for the last-minute decisions during the contest.

Another critical aspect, that is worth to be discussed, is related to the weather data. The typical meteorological year that was used for initial simulations at the design phase resulted to be distant from the real weather conditions during the contest season. In fact, the real weather was hotter, more humid, and the sky was more covered (2 raining days) than simulated and therefore the

power needed for the cooling was higher, with higher consumption too, and the electricity production less than expected.

The monitored weather data implemented in the final simulations with the calibrated model, as well as the safety range considered for the sizing and the performance assessment of the cooling system, resulted to be good strategies to keep the model close to the reality, thus confirming the strength of the optimization.

4. Conclusion

This work presents an effective transition from theoretical simulation and optimization methods to their experimental applications in reality and back. It has been demonstrated that simulation-based optimization approaches, which are currently being developed and mainly used for research purpose, can successfully support the entire process and add significant value to the resulting ZEB. In fact, despite the highlighted difficulties in the transition from theory to practice and from design to operation, mainly due to time constraints, they greatly helped optimize the performance of the ZEB prototype and win the Solar Decathlon China 2018 competition, demonstrating their applicability and scalability to real contexts.

This multi-step approach may be replicated to optimize the role of simulation-based optimization in a real building design, construction and management process. In fact, the optimization-aided calibration offered a good range of available codes for performing the final simulation, giving the opportunity to pick the one that better suits the simulation and to tailor it to the specifics of the wanted calibration. The results have given a substantial help to the monitoring and planning system and have shown the flexibility of the calibration procedure in reshaping itself according to the building site and operational needs.

The multi-stage calibration approach has been used to ensure the simulation model reflects the different steps of the building construction phase and the building behavior. It has resulted to be effective in reaching good results while maintaining the model physically realistic and manageable. We believe this approach can be useful to be replicated on other buildings, provided a sensitivity analysis is performed to select a proper set of calibration parameters.

Concerning the final combined design and operational optimization approach, the achieved time saving with respect to the manual comparison of different combination of variables is important, considering that the number of analyzed design and operation alternatives is huge and that unexpected design solution may emerge from the automated process.

Further, most of the resulting optimal design parameters were implemented in the construction of the house, while others were used to drive the prototype monitoring and management. In this

way, it has been possible to have the best overall analysis, both for the design and management phases, and win the competition. The optimization work led to improve the contest score by more than 15 points with respect to the estimated score pre-optimization. This adds even more value to the work itself, in a context where a single point can change the outcome of the competition and the competition was won with a deviation less than 12 points with respect to the second team.

As a general conclusion, it has emerged that the accuracy of the model has a great influence on the results and therefore on the effectiveness of the approach. In particular, the iterative model calibration and optimization is fundamental to reach high performance levels. The test of the building behavior by means of the calibrated model was useful to prevent unexpected errors in the contest measurements and to predict the future building behavior. Also, a tailored sensitivity analysis can help refine the variables mesh of variation and prioritize the correct implementation of the resulting optimal strategies if external constraints (e.g. time, budget, ..) occur and will be investigated in future work.

The presented method can be applied to other prototypes, to building fine-testing, to support commissioning. It can be further applied for other competitions or for supporting the transition to market of the Solar Decathlon prototypes.

Acknowledgement

This work has been performed as part of the activities of the team SCUT-POLITO (South China University of Technology, Guangzhou, China – Politecnico di Torino, Turin, Italy), winner of the Solar Decathlon China 2018 contest (http://www.sdchina2017-scutpolito.com).

The contribution of all the students composing the team from Italy and China is acknowledged, as well as the contribution of the team leader Yicheng Wang in providing comments to the final draft of the paper. The team was supervised by the followings:

SCUT professors: Yimin Sun, Yiqiang Xiao, Jing Wang, Haohao Xu, Yufeng Zhang, Guanqiu Zhong, Lei Xiao.

PoliTo professors: Mauro Berta (Scientific coordinator, DAD), Michele Bonino (DAD), Orio De Paoli (DAD), Enrico Fabrizio (DENERG), Marco Filippi (DENERG), Francesca Frassoldati (DAD), Matteo Robiglio (DAD), Valentina Serra (DENERG), Edoardo Bruno (DAD).

LINKS-SiTI research group: Romano Borchiellini (DENERG), Sergio Olivero, Paolo Lazzeroni, Federico Stirano.

AUTHOR STATEMENT

Maria Ferrara: Conceptualization, Methodology, Software, Writing- Original draft preparation, Reviewing and Editing. **Ciro Lisciandrello**: Investigation, Data curation, Writing- Original draft preparation. **Alessio Messina**: Investigation, Data curation, Writing- Original draft preparation. **Mauro Berta:** Supervision, project administration**.** **Yufeng Zhang**: Supervision, project administration. **Enrico Fabrizio:** Conceptualization, Methodology, Supervision.

DECLARATION OF INTEREST

We wish to confirm that there are no known conflicts of interest associated with this publication and there has been no significant financial support for this work that could have influenced its outcome.

We confirm that the manuscript has been read and approved by all named authors and that there are no other persons who satisfied the criteria for authorship but are not listed. We further confirm that the order of authors listed in the manuscript has been approved by all of us.

We confirm that we have given due consideration to the protection of intellectual property associated with this work and that there are no impediments to publication, including the timing of publication, with respect to intellectual property. In so doing we confirm that we have followed the regulations of our institutions concerning intellectual property.

We understand that the Corresponding Author is the sole contact for the Editorial process (including Editorial Manager and direct communications with the office). He/she is responsible for communicating with the other authors about progress, submissions of revisions and final approval of proofs. We confirm that we have provided a current, correct email address which is accessible by the Corresponding Author and which has been configured to accept email from.

References

[1] Torcellini, P., Crawley, D. Understanding Zero-Energy Buildings. *ASHRAE Journal* **2006**, *48*, 62-69.

[2] Barone, G., Buonomano, A., Calise, F., Forzano, C., Palombo, A. Building to vehicle to building concept toward a novel zero energy paradigm: Modelling and case studies. *Renewable and Sustainable Energy Reviews* **2019**, 625-648.

[3] Ferrara, M.; Monetti, V.; Fabrizio, E. Cost-Optimal Analysis for Nearly Zero Energy Buildings Design and Optimization: A Critical Review. *Energies* **2018**, *11*, 1478.

[4] Ferrara, M., Fabrizio, E., Virgone, J., Kuznik, F., Filippi, M. Modelling Zero Energy buildings: parametric studies for the technical optimization. *Energy Procedia* **2014**, *62*, 200-209.

[5] Evins R. A review of computational optimization methods applied to sustainable building design, *Renewable and Sustainable Energy Reviews* **2013**, *22*, 230–245.

[6] Lin, B., Yu, Q., Li, Z., Zhou, X. Research on parametric design method for energy efficiency of green building in architectural scheme phase. *Frontiers of Architectural Research* **2013**, *2(1),* 11-22.

[7] Li, K. Pan, L., Xue, W., Jiang, H., Mao, H. Multi-Objective Optimization for Energy Performance Improvement of Residential Buildings: A Comparative Study. *Energies* **2017**, *10(2)*, 245.

[8] Wu, W., Guo, J., Li, J., Hou, H., Meng, Q., Wang, W. A Multi-objective Optimization Design Method in Zero Energy Building Study: A Case Study Concerning Small Mass Buildings in Cold District of China. *Energy and Buildings* **2018,** *158,* 1613-1624

[9] Ferrara, M., Sirombo, E., Fabrizio E. Automated optimization for the integrated design process: the energy, thermal and visual comfort nexus, *Energy and Buildings* **2018**, *168,* 413-427.

[10] Hernandez, P., Kenny, P. From net energy to zero energy buildings: Defining life cycle zero energy buildings (LC-ZEB), *Energy and Buildings* **2010**, *42(6)*, 815 – 821.

[11] Ferrara, M, Sirombo, E., Fabrizio, E. Energy-optimized versus cost-optimized design of high- performing dwellings: The case of multifamily buildings. *Science and Technology for the built environment* **2018**, *24(5)*, 513-528.

[12] Ikeda, S., Choi, W., Ooka, R. Optimization method for multiple heat source operation including ground source heat pump considering dynamic variation in ground temperature. *Applied energy* **2017**, *193*, 466-478.

[13] Burak Gunay, H., Ouf, M., Newsham, G., O'Brien, W. Sensitivity analysis and optimization of building operations, *Energy and Buildings* **2019**, *199,* 164-175.

[14] Thieblemont, H., Haghighat, F., Ooka, R., Moreau, A. Predictive control strategies based on weather forecast in buildings with energy storage system: A review of the state-of-the art. *Energy and Buildings* **2017**, *153*, 485-500

[15] Wilde, P. The gap between predicted and measured energy performance of buildings: A framework for investigation. *Automation in Construction* **2014**, *41*, 40–49.

[16] Fabrizio, E., Monetti, V. Methodologies and Advancements in the Calibration of Building Energy Models. *Energies* **2015** *8*, 2548-2574.

[17] Clarke, J.A.; Strachan, P.; Pernot, C. An approach to the calibration of building energy simulation models. *ASHRAE Transactions* **1993,** *99*, 917–927.

[18] Ferrara, M.; Rolfo, A.; Prunotto, F.; Fabrizio, E. EDeSSOpt—Energy Demand and Supply Simultaneous Optimization for cost-optimized design: Application to a multi-family building. *Applied Energy* **2019**, *236*, 1231–1248.

[19] Yang, T., Pan, Y., Mao, J., Wang, Y., Huang, Z. An automated optimization method for calibrating building energy simulation models with measured data: Orientation and a case study. *Applied Energy* **2016**, *179*, 1220-1231.

[20] Tian, W. A review of sensitivity analysis methods in building energy analysis. *Renewable and Sustainable Energy Reviews* **2013**, *20*, 411-419.

[21] Fantozzi, F., Leccese, F., Salvadori, G., Spinelli, N., Moggio, M., Pedonese, C., Formicola, L., Mangiavacchi, E., Baroni, M., Vegnuti, S., Baldanzi, V., Fontani, M., Mori, G., Forassiepi, R. Solar Decathlon ME18 competition as a 'learning by doing' experience for students: The case of the team HAAB. *IEEE Global Engineering Education Conference*, EDUCON, **2018,** 1865-1869.

[22] https://www.davisinstruments.com/solution/vantage-pro2/

[23] https://www.deltaohm.com/en/wp-content/uploads/document/DeltaOHM-HD2102.1_2-Luxmeter-Datalogger-Datasheet-en.pdf

[24] http://www.deltaohm.com/ver2012/download/LP_PYRA02_03_12_uk.pdf

[25] Royapoor, M., Roskilly, T. Building model calibration using energy and environmental data, *Energy and buildings* **2015**, *94*, 109-120.

[26] https://www.onsetcomp.com/datasheet/U23-001

[27] Raftery, P., Keane, M., O'Donnell, J. Calibrating whole building energy models: An evidence-based methodology. *Energy and Buildings* **2011**, *43*, 2356-2364.

[28] Enríquez, R., Jiménez, M.J., Heras, M. Analysis of a Solar Office Building at the South of Spain Through Simulation Model Calibration, *Energy Procedia* **2012**, *30*, 580-589.

[29] Fabriek, P.H. Sensitivity analysis of residential building simulations: model choice for specific applications and critical parameters. *Master thesis*, **2013**, TU Delft.

[30] Nguyen, A., Reiter, S. A performance comparison of sensitivity analysis methods for building energy models. *Building simulation* **2015,** *8*, 651-664.

[31] Morris, M. D. Factorial Sampling Plans for Preliminary Computational Experiments. *Technometrics* **1991**, *33*, 161-174.

[32] Saltelli, A., Ratto, M., Campolongo, F., Andres, T., Tarantola, S. Global Sensitivity Analysis. **2008.** The Primer. John Wiley and Sons. Chichester (UK).

[33] Campolongo, F., Cariboni, J., Saltelli, A. An effective screening design for sensitivity analysis of large models. *Environmental Modelling & Software* **2007**, *22*, 1509-1518.

[34] Wetter, M. GenOpt Generic Optimization Program User Manual, v3.1.0, **2011**.

[35] Kennedy, J and Eberhart, R.C. Particle swarm optimization. In *IEEE International Conference on Neural Networks* **1995**, *vol. IV*, 1942–1948.

[36] Kennedy, J. and Eberhart, R.C. A discrete binary version of the particle swarm algorithm. IEEE Proc. of Systems, Man, and Cybernetics **1997**, *5*, 4104–4108.

[37] Machairas, M. Tsangrassoulis, A., Axarli, K. Algorithms for optimization of building design: A review, *Renewable and Sustainable Energy Reviews* **2014,** *31*, 101-112.

[38] Ferrara, M, Dabbene, F., Fabrizio, E. Optimization Algorithms Supporting The Cost-Optimal Analysis: The Behavior of PSO. *Proceedings of BS 2107*, **2017**, San Francisco, USA.

[39] Waibel, C., Wortmann, T., Evins, R., Carmeliet, J. Building energy optimization: An extensive benchmark of global search algorithms, *Energy and Buildings*, **2019**, *187*, 218-240.